

MICROTECHNOLOGY AND MEMS

F. Li
A. Nathan

CCD Image Sensors in Deep-Ultraviolet

Degradation
Behavior and
Damage Mechanisms

 Springer

MICROTECHNOLOGY AND MEMS

MICROTECHNOLOGY AND MEMS

Series Editor: H. Baltes H. Fujita D. Liepmann

The series Microtechnology and MEMS comprises text books, monographs, and state-of-the-art reports in the very active field of microsystems and microtechnology. Written by leading physicists and engineers, the books describe the basic science, device design, and applications. They will appeal to researchers, engineers, and advanced students.

Mechanical Microsensors

By M. Elwenspoek and R. Wiegerink

CMOS Cantilever Sensor Systems

Atomic Force Microscopy and Gas Sensing Applications

By D. Lange, O. Brand, and H. Baltes

Micromachines as Tools for Nanotechnology

Editor: H. Fujita

Modelling of Microfabrication Systems

By R. Nassar and W. Dai

Laser Diode Microsystems

By H. Zappe

Silicon Microchannel Heat Sinks

Theories and Phenomena

By L. Zhang, K.E. Goodson, and T.W. Kenny

Shape Memory Microactuators

By M. Kohl

Force Sensors for Microelectronic Packaging Applications

By J. Schwizer, M. Mayer and O. Brand

Integrated Chemical Microsensor Systems in CMOS Technology

By A. Hierlemann

CCD Image Sensors in Deep-Ultraviolet

Degradation Behavior and Damage Mechanisms

By F.M. Li and A. Nathan

F.M. Li
A. Nathan

CCD Image Sensors in Deep-Ultraviolet

Degradation Behavior
and Damage Mechanisms

With 84 Figures

 Springer

Flora M. Li
Arokia Nathan
Electrical & Computer Engineering
University of Waterloo
Waterloo, Ontario N2L 3G1
Canada
Emails: fmli@uwaterloo.ca
anathan@uwaterloo.ca

Series Editors:

Professor Dr. H. Baltes
ETH Zürich, Physical Electronics Laboratory
ETH Hoenggerberg, HPT-H6, 8093 Zürich, Switzerland

Professor Dr. Hiroyuki Fujita
University of Tokyo, Institute of Industrial Science
4-6-1 Komaba, Meguro-ku, Tokyo 153-8505, Japan

Professor Dr. Dorian Liepmann
University of California, Department of Bioengineering
466 Evans Hall, #1762, Berkeley, CA 94720-1762, USA

ISSN 1439-6599

ISBN 3-540-22680-X Springer Berlin Heidelberg New York

Library of Congress Control Number: 2004116223

This work is subject to copyright. All rights are reserved, whether the whole or part of the material is concerned, specifically the rights of translation, reprinting, reuse of illustrations, recitation, broadcasting, reproduction on microfilm or in any other way, and storage in data banks. Duplication of this publication or parts thereof is permitted only under the provisions of the German Copyright Law of September 9, 1965, in its current version, and permission for use must always be obtained from Springer. Violations are liable to prosecution under the German Copyright Law.

Springer is a part of Springer Science+Business Media

springeronline.com

© Springer-Verlag Berlin Heidelberg 2005

Printed in The Netherlands

The use of general descriptive names, registered names, trademarks, etc. in this publication does not imply, even in the absence of a specific statement, that such names are exempt from the relevant protective laws and regulations and therefore free for general use.

Typesetting: by the authors and TechBooks using a Springer \LaTeX macro package

Cover concept: eStudio Calamar Steinen

Cover production: *design & production* GmbH, Heidelberg

Printed on acid-free paper 57/3141/jl - 5 4 3 2 1 0

Preface

As the deep-ultraviolet (DUV) laser technology continues to mature, an increasing number of industrial and manufacturing applications are emerging. For example, the new generation of semiconductor inspection systems are being pushed to image at increasingly shorter DUV wavelengths to facilitate inspection of deep sub-micron features in integrated circuits. DUV-sensitive charge-coupled device (CCD) cameras are in demand for these applications. Although CCD cameras that are responsive at DUV wavelengths are now available, their long-term stability is still a major concern. Since the energy of DUV photons is comparable to the band-gap energy of the silicon dioxide (SiO_2), photoreactions can occur in the SiO_2 layer of the CCD image sensor and introduce anomalous behavior.

Given the relative infancy of research in CCD-DUV interactions, publications in this area are somewhat sporadic. This book describes the degradation mechanisms and long-term performance of CCDs. The material presented in this book evolves from a comprehensive literature survey of the scientific research that underpins degradation behavior of CCDs.

Part I begins with an overview of CCD image sensors, and addresses the issues concerning CCD imaging in DUV, along with the common UV enhancement techniques adopted by the industry. Currently, backside-thinned back-illuminated CCD cameras are the leading contender from the standpoint of UV sensitivity. However, such cameras are expensive, and are vulnerable to radiation-induced instability, similar to other CCD designs. To understand the origins of CCD instability in DUV, knowledge of the reliability issues of the silicon-silicon dioxide (Si-SiO_2) system is essential. In Part II, the properties of Si, SiO_2 , and Si-SiO_2 interface are described. On irradiation, the Si substrate, the SiO_2 layer, and the Si-SiO_2 interface interact with the incoming photons resulting in damage introduced to the CCD sensor. A discussion of the general effects of radiation is presented in Part III, where we consider the different types of defects and reactions that can arise in the Si-SiO_2 structures. Material interactions with UV radiation are examined in Part IV to identify the sources of instability in CCDs. Part V introduces experimental data that characterize thinned front-illuminated linear CCD sensors, when subjected to F_2 ($\lambda = 157 \text{ nm}$) excimer laser irradiation. Mechanisms responsible for the DUV-induced degradation behavior in CCD sensors are

identified. Because the mechanisms are associated with the Si-SiO₂ system, the analysis can also be extended to other silicon-based UV sensor architectures. Potential design optimization techniques to improve the quantum efficiency (QE) and stability of CCD sensors at DUV wavelengths are discussed in Part VI, followed by concluding remarks and recommendations for future research. A better understanding of the mechanisms underlying DUV-induced degradation of CCD sensors can assist in the design and development of new-and-improved DUV-sensitive CCD sensors.

This work was supported by DALSA Corporation, University of Waterloo, and the Natural Sciences and Engineering Research Council (NSERC) of Canada. The authors acknowledge the contributions by Dr. Nixon O at DALSA Corporation, for his support and the numerous stimulating discussions.

Waterloo, ON, Canada
December 2004

Flora M. Li
Arokia Nathan

Contents

1	Introduction	1
1.1	Motivation: CCD for DUV Imaging	2
1.2	Outline of the Book	3

Part I CCD Image Sensors

2	Overview of CCD	7
2.1	Fundamentals of Solid-State Imaging	11
2.1.1	Absorption of Photons	11
2.1.2	Charge Collection	13
2.2	CCD Response and Quantum Efficiency	14
2.2.1	Spectral Response	14
2.2.2	Quantum Efficiency (QE)	15
2.2.3	Pixel Response Non-Uniformity (PRNU)	17
2.3	Dark Current	17
2.3.1	Basics of Dark Current	18
2.3.2	Sources of Dark Current	18
2.3.3	Dark Signal Non-Uniformity (DSNU)	19
2.4	Charge Conversion Efficiency (CCE) and Output Node	20
3	CCD Imaging in the Ultraviolet (UV) Regime	23
3.1	Ultraviolet (UV) Spectrum	24
3.2	Applications of CCD in DUV	27
3.2.1	Photolithography	27
3.2.2	Microstructure Generation	29
3.2.3	Wafer Inspection System	30
3.2.4	Beam Profiler for Laser System	31
3.2.5	DUV Microscope	31
3.2.6	Spectroscopy	32
3.3	Techniques to Improve UV Sensitivity	33
3.3.1	Virtual-Phase CCDs and Open-Electrode CCDs	33
3.3.2	Backside-Thinned Back-Illuminated CCDs	35

3.3.3	UV-Phosphor Coated CCDs	38
3.3.4	Deep-Depletion CCDs	39
3.3.5	Other UV Enhancement Techniques	39
3.4	Challenges of DUV Detection Using CCDs	40

Part II Instabilities in Si, SiO₂, and the Si-SiO₂ Interface

4	Silicon	45
4.1	Optical Properties of Si	45
4.1.1	Photoelectric Effect and Si	45
4.2	Defects in Si	48
4.3	Si Wafers for CCDs	49
5	Silicon Dioxide	51
5.1	Basic Properties of SiO ₂	51
5.1.1	Structural Properties of SiO ₂	51
5.1.2	Optical Properties of SiO ₂	54
5.2	Defects in SiO ₂	54
5.2.1	Physical Nature of Defects in SiO ₂	56
5.2.2	Formation Reactions of Defects in SiO ₂	65
5.2.3	Behavior of SiO ₂ Defects in Si-SiO ₂ System	67
5.3	Instability in Si-Based Devices due to Defects in SiO ₂	74
5.3.1	Reliability Issues due to Optically-Active Defects in SiO ₂	75
5.3.2	Reliability Issues due to Electrically-Active Defects in SiO ₂	76
5.3.3	Instability in MOSFETs due to Electrically-Active Defects	77
6	Si-SiO₂ Interface	81
6.1	Physical Structure of the Si-SiO ₂ Interface	81
6.2	Defects at the Interface	82
6.2.1	Formation of Interface States	83
6.2.2	Carrier Exchange at Interface States	86
6.2.3	Models of Interface Defects	86
6.2.4	Electrically-Active Defects at the Si-SiO ₂ Interface ...	90

Part III Effects of Radiation on the Si-SiO₂ System

7	General Effects of Radiation	95
7.1	Overview of Radiation Effects on Matter	95

7.1.1	Displacement Damage	96
7.1.2	Ionization Damage	96
7.1.3	Interactions of Photons with Matter	98
7.2	Radiation-Induced Defects in Si, SiO ₂ , and Si-SiO ₂ Interface	99
7.2.1	Radiation-Induced Defects in Si	100
7.2.2	Radiation-Induced Defects in SiO ₂	100
7.2.3	Radiation-Induced Defects in Si-SiO ₂ Interface	102
7.3	Effects of Radiation on Basic Semiconductor Devices	102
7.3.1	Radiation Effects on MOS Structures	103
7.3.2	Radiation Effects on Electro-Optical Devices	107
7.3.3	Annealing of Radiation-Induced Defects	107
7.3.4	Radiation Hardening	107
8	Effects of Radiation on CCDs	109
8.1	Overview of the Radiation Damages in CCDs	109
8.2	Ionization Damage in CCDs	111
8.2.1	e-h Generation	112
8.2.2	e-h Recombination and Fractional Yield	112
8.2.3	Hole Transport	113
8.2.4	Hole Trapping	113
8.2.5	Annealing (Detrapping of Holes)	114
8.2.6	Interface State Creation	114
8.2.7	Dependence of Ionization Damage on Insulator Properties	116
8.2.8	UV Flood	117

**Part IV Interaction of UV Radiation
with the Si-SiO₂ System**

9	UV-Induced Effects in Si	121
9.1	Photoemission in Si	121
10	UV Laser Induced Effects in SiO₂	125
10.1	Overview of UV Laser Induced Effects in SiO ₂	126
10.1.1	Color Center Formation and Induced Absorption	127
10.1.2	Density Change	128
10.1.3	Photorefractive Effect	129
10.2	Active Defects in DUV	129
10.2.1	Oxygen-Deficient Centers (ODCs)	130
10.2.2	E' Centers	131
10.2.3	Non-Bridging Oxygen Hole Centers (NBOHCs)	132
10.3	KrF and ArF Laser Induced Effects in SiO ₂	133

10.3.1	Wavelength vs. Rate of Color Center Formation	133
10.3.2	Induced Absorption due to KrF Excimer Laser Radiation	134
10.3.3	Induced Absorption due to ArF Excimer Laser Radiation	135
10.3.4	Fluctuations in UV-Induced Absorption	136
10.4	F ₂ Laser Induced Effects in SiO ₂	138
10.4.1	F ₂ Laser Induced Defect Formation in SiO ₂	139
10.4.2	Dependence of Defect Formation on F ₂ Laser Power . .	141
10.4.3	F ₂ Laser Induced Bleaching of the VUV Absorption Edge	145
10.5	UV-Induced Charging of SiO ₂	147
10.6	Summary of the UV-Induced Effects in SiO ₂	150
10.6.1	Optical	150
10.6.2	Electrical	151
11	UV Laser Induced Effects at the Si-SiO₂ Interface	153

**Part V Interaction of DUV Radiation
with CCD Sensors**

12	CCD Measurements at 157 nm	157
12.1	Experiment Description	157
12.1.1	Laser Setup	157
12.1.2	Frontside-Thinned Front-Illuminated CCDs	159
12.1.3	Laser Exposure Conditions	161
12.2	Experimental Results	162
12.2.1	Response Measurement of Sample-A at 157 nm	162
12.2.2	Response Measurement of Sample-B at 157 nm	164
12.2.3	Higher Intensity 157 nm Exposure on Sample-A: Accelerated Degradation Testing	166
12.2.4	Higher Intensity 157 nm Exposure on Sample-B: Dark Current Measurement	168
12.3	Analysis of DUV Damage Mechanisms	169
12.3.1	Analysis of 157 nm Response Measurements	170
12.3.2	Analysis of Dark Current Measurements	176
12.4	Post-157 nm Measurements	177
12.4.1	Dark Current Response of Sample-A After 157 nm Irradiation	178
12.4.2	Dark Current Response of Sample-B After 157 nm Irradiation	180
12.4.3	DUV-Induced Changes in Visible QE of Sample-A . . .	181
12.4.4	DUV-Induced Changes in Visible QE of Sample-B . . .	182

12.4.5 DUV-Induced Changes in CCE 186
 12.5 Response Measurement of Photodiodes at 157 nm 187
 12.6 Summary of CCD Behavior at 157 nm 190
 12.7 Future Investigations 191

Part VI Concluding Remarks & Future Research

13 Design Optimizations for Future Research 195
 13.1 Optimization Techniques Based
 on UV Photodiodes 196
 13.1.1 Characteristics of Photodiodes in UV 196
 13.1.2 Techniques to Improve the UV Performance 198
 13.2 Optimization Techniques Based
 on DUV Silica Glass 206

14 Concluding Remarks 207
 14.1 Conclusions 207
 14.2 Recommendations 208

Glossary and Definition of Acronyms 211

References 223

Index 229

1 Introduction

As charge-coupled device (CCD) technology matures, its dominance in the digital imaging market for both the consumer and industrial sectors continues to grow [1]. Although commercial digital cameras have a minimal need for ultraviolet (UV) sensitivity, UV-responsive cameras are in demand for industrial and manufacturing applications. Examples include manufacturing inspection systems, UV spectroscopy, and astronomical applications. More recently, the need for CCD imaging has been extended to even shorter wavelengths in the deep-UV (DUV) spectrum. One of the key applications of CCDs in DUV is to facilitate the inspection of deep sub-micron features and defects of wafers and photomasks in semiconductor inspection systems. Therefore, DUV-sensitive CCD cameras with high-speed, high-resolution, and digital imaging capabilities are crucial for these wafer inspection systems.

However, the development of CCD cameras with a high UV responsivity and long-term stability is not straightforward. Conventional CCD image sensor architectures are usually insensitive to UV radiation (10 to 400 nm). This is because CCD sensors are typically built with silicon technology, and the absorption depth of photons in silicon decreases exponentially as the wavelength decreases. This makes the charge collection in the silicon depletion region extremely difficult. In addition, a large portion of the incident UV photons are absorbed by the frontside gate structure for photogate-based CCD sensors. The polycrystalline silicon (abbreviated as polysilicon) gate material in conventional photogate-based CCDs is at least 400 nm thick, whereas its penetration depth for 400 nm radiation is only 2 nm [2]. Thus, the polysilicon gate effectively shields the active regions of the CCD sensor from incident UV radiation, causing a significant reduction in the quantum efficiency (QE). The gate oxide and passivation layers which are composed of SiO_2 can be another source of interference for the incoming UV photons because the SiO_2 becomes absorbent at UV wavelengths. This situation further deteriorates as the wavelength decreases into the DUV spectrum and below it. As the use of CCD sensors becomes more ubiquitous in manufacturing and lithographic applications, it is critical to develop CCD cameras with a reasonable responsivity and stability for the detection of DUV radiation with shorter wavelengths (higher energies).

1.1 Motivation: CCD for DUV Imaging

One of the main driving forces behind developing CCD sensors for DUV imaging is the continually evolving interest for finer resolution in semiconductor manufacturing. The increasing demands for a higher integration density of integrated circuits (ICs) require device fabrication tools that exploit shorter wavelength illuminations for optical lithography. In these manufacturing applications, the very short wavelengths of DUV light allow the fabrication of devices with dimensions in the deep sub-micron regime. Although wafer production systems with the illumination sources of 248 nm and 193 nm are well established, lithography with 157 nm (F_2) fluorine excimer laser is emerging as a viable technology for the post-193 nm era. In fact, in the year of 2000, the semiconductor industry forecasted 157 nm F_2 excimer laser to be the technology of choice for feature sizes in the 100 nm to 70 nm nodes, and anticipated the appearance of F_2 excimer laser in a new generation of optical lithography systems by 2005 [3, 4]. 157 nm lithography is attractive for several reasons; the pivotal reason is that it is an extension of the existing optical lithography systems which has longer DUV wavelengths of 248 nm and 193 nm. Therefore, it is possible to adapt the existing manufacturing and wafer-processing infrastructures to 157 nm lithography systems. In addition, optical resolution enhancing techniques (e.g., phase-shifting masks and off-axis illumination) used in the current generation of lithography systems can be extended to the new generation of 157 nm systems. However, with the recent advancements in immersion-based 193 nm lithography tools demonstrating image resolutions down to 45 nm node and below, the introduction of 157 nm lithography systems in production lines will likely be delayed [5–7]. The 193 nm immersion lithography is predicted to become the toolset of choice for the 65 nm and 45 nm nodes on the semiconductor industry roadmap; those nodes are slated to enter production in 2007 and 2009, respectively [7].

The transition to the 157 nm wavelength is expected to encounter challenges comparable to those of earlier shifts in the lithography wavelength from 365 nm (i-line) to 248 nm, and from 248 nm to 193 nm. Some of the critical issues include the availability of the optical materials and coatings, the mask materials and pellicles, a controlled ambience to minimize contamination of the optical surfaces, as well as compatible sensors and detection devices optimized for 157 nm imaging applications [3]. An example of a sensing device commonly found in mask/wafer inspection and monitoring modules of the lithographic manufacturing systems is the CCD camera. For the reliable operation of manufacturing and inspection systems, CCD sensors must maintain a high sensitivity and stability when they are exposed to DUV. Therefore, the performance of CCD sensors in the DUV regime is one of the many factors that shapes the evolution to DUV lithography. With engineers currently developing production technology for the 90 nm and 65 nm nodes in various wafer fabs, there have been real concerns for the first time where these development engineers lack the needed inspection and metrology

technologies at the start of their development work. Thus, the industry requires some breakthroughs that solve the natural limitations to conventional CCD and laser scanning inspection technology at DUV wavelengths [8].

In addition to lithography and semiconductor inspection, numerous other applications can benefit from the development of DUV-sensitive CCD imagers.¹ Therefore, CCD cameras that are sensitive in the DUV must be developed to keep up with the advancements in lithography and in other industrial applications.

1.2 Outline of the Book

DUV-sensitive CCD cameras that are fast, responsive, and stable are desirable for a growing number of industrial applications that requires DUV imaging capability. However, conventional CCD cameras respond poorly in DUV because the frontside polysilicon and oxide structures absorb UV photons, and the absorption depth of UV photons in silicon is short. Moreover, high-energy UV photons can cause irreparable damage to conventional CCD cameras. It is possible to eliminate the use of polysilicon layers in certain CCD architectures (e.g., photodiode-based CCDs) so that the UV problems introduced by the polysilicon can be dismissed. However, the presence of oxide (SiO_2) layers is imperative for any silicon-based CCD structure. Thus, consideration must be given to the properties of the SiO_2 layer when CCD sensors are designed for DUV wavelengths.

The use of CCD image sensors at DUV wavelengths has been investigated by a few groups [9, 10]. Although CCD cameras that are responsive in the DUV are now available, their long-term stability is still a major concern. Despite CCD instability issues, there are very few publications in the scientific literature that address the long-term performance, radiation tolerance, or the causes of degradation of CCDs after exposure to DUV wavelengths. These are the motivations for developing new CCD structures that are optimized for DUV imaging applications, and for thoroughly investigating the DUV damage mechanisms in CCDs.

Following the introduction, an overview of CCD image sensors is provided in Part I, which encompasses a discussion on issues concerning CCD imaging in DUV and examples of UV enhancement techniques exercised by the industry. Currently, the backside-thinned back-illuminated CCD camera is the leading contender for offering the highest UV sensitivity; however, such a camera is the most expensive and it suffers from radiation-induced instabilities similar to those experienced by most other CCD structures.

To understand and recognize the origins of CCD instabilities in the DUV, a general knowledge of the reliability issues of the Si-SiO₂ system is essential. Part II is a discussion of the basic properties and defects of silicon (Si), silicon

¹Refer to Chap. 3 for examples of CCD applications in DUV.

dioxide (SiO_2), and Si-SiO₂ interface. On irradiation, the Si substrate, the SiO₂ layer and the Si-SiO₂ interface can interact with incoming photons to subject the CCDs to a variety of effects or damage. Part III discusses the general effects of radiation on Si-SiO₂ system and on CCDs. This provides the background to understand the type of defects and reactions that can arise from radiation in Si-SiO₂ materials. Material interactions with UV radiation are considered in Part IV to build a foundation for studying the causes of the instabilities in CCDs specifically at DUV wavelengths. The findings gathered from the various scientific research areas are assembled to identify the mechanisms of the CCD behavior in DUV.

In addition to understanding instabilities, a new and more economical technique that enhances the DUV sensitivity of frontside-illuminated linear CCDs is introduced. This technique involves thinning the overlying oxide on the top of the imaging area (i.e., the photodiode) of the linescan sensor to reduce the absorption of the DUV photons in the SiO₂ layer. For simplicity, the discussion of thinned front-illuminated sensors here is confined to CCD structures with no polysilicon on the imaging region; namely, photodiode-based linear CCD architecture. As a result, the research focuses on the concerns associated with the DUV-induced effects in the SiO₂ layer, not the issues that can arise from the polysilicon layer. The characterization of this frontside-thinned front-illuminated linear CCD structure at the DUV wavelength of 157 nm is presented in Part V. By using the theories presented in the preceding chapters, the possible causes and origins of the observed CCD behavior in DUV are revealed. A better understanding of the mechanisms behind the DUV-induced degradation of CCD sensors can assist in the design and development of new-and-improved DUV-sensitive CCD sensors in the future. Finally, the significance of the findings of the research in this book are summarized and future research activities are suggested.

Part I

CCD Image Sensors

2 Overview of CCD

CCD is the abbreviation for *charge-coupled device*. CCD image sensors are silicon-based integrated circuits (ICs), consisting of a dense matrix of photodiodes or photogates that operate by converting light energy, in the form of photons, into electronic charges [11]. For example, when an UV, visible or infrared (IR) photon strikes a silicon (Si) atom in or near a CCD photosite, the photon usually produces a free electron and a hole via the photoelectric effect. The primary function of the CCD is to collect the photogenerated electrons in its “potential wells” (or pixels) during the CCD’s exposure to radiation, and the hole is then forced away from the potential well and is eventually displaced into the Si substrate. The more light that is incident on a particular pixel, the higher the number of electrons that accumulate on that pixel. By varying the CCD gate voltages, the depth of the potential wells can be modified. This action enables the transfer of the photogenerated electrons across the registers to the “read-out” circuit. The output signal is then transferred to the computer for image regeneration or image processing. Figure 2.1 denotes that a typical CCD sensor consists of a sandwich of semiconductor layers that are overlaid with a network of gates (or electrodes) to control the transfer of the signal charges from the pixels to the read-out circuitry at the output node [11].

The pixels in a CCD sensor can be arranged in various configurations. Figure 2.2 displays two classic CCD architectures: a linear CCD and an area array CCD. A linear (or linescan) CCD sensor consists of a single line of pixels, adjacent to a CCD shift register that is required for the read-out of the charge packets. The isolation between the pixels and the CCD register is achieved by a transfer gate. Typically, the pixels of a linear CCD are formed by the photodiodes. The CCD shift register is composed of a series of MOS (metal-oxide-semiconductor) capacitors arranged closely across the Si wafer so that the charge can be moved from one capacitor to the next as efficiently as possible. The MOS capacitors are formed by depositing a highly conductive layer of polysilicon on top of the insulating layer of silicon dioxide (SiO_2) that covers the Si substrate [11]. Figure 2.1 provides a cross-sectional view of a linescan CCD sensor.

After the integration of the charge carriers in the photodiodes (i.e., the exposure period), the transfer gate is raised to a high voltage to simultaneously

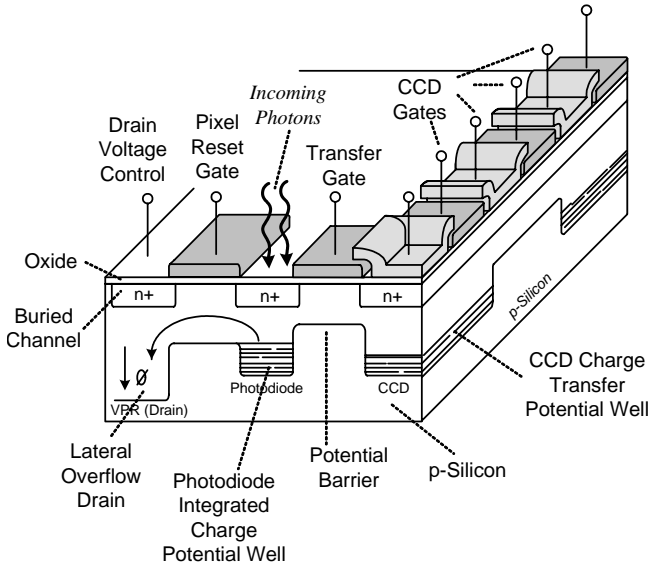


Fig. 2.1. The anatomy of a CCD sensor. The configuration corresponds to a photodiode-based linear CCD (adapted from [11])

transfer the charges in all the pixels in a parallel manner toward the CCD shift register, as indicated by the arrows in Fig. 2.2(a). When the transfer gate voltage returns to its off state, a new integration period begins. At the same time, the charge packets are transferred through the CCD shift register toward the output of the device in a serial fashion. The CCD shift register must be shielded from the incoming light to avoid disturbing the number of carriers in the charge packet [12]. During the imaging operations, the linear CCD sensor is placed along a single axis so that the scanning occurs in only one direction. A line of information from the scene is captured at each integration period, and subsequently read out of the device before stepping to the next line index. An example of linescan imaging is the fax machine. For the purpose of the study in this book, photodiode-based linescan CCDs are used for the DUV experiments in Chap. 12.

Two-dimensional imaging is possible with area array CCD sensors; the entire image is captured with one exposure, eliminating the need for any movement by the sensor or the scene. An example of a compact and simple full-frame area sensor is illustrated in Fig. 2.2(b). The area sensor is composed of an array of photogates (i.e., MOS photocapacitors) that provide both the charge collection and charge transfer functionalities for the CCD sensor. The gate electrode of the photogate is fabricated from polysilicon. A set of parallel light-sensitive CCD registers that is composed of photogates is oriented vertically and is denoted as the vertical CCD registers (VCCD). A simple cross-sectional view of a photogate-based CCD register is depicted

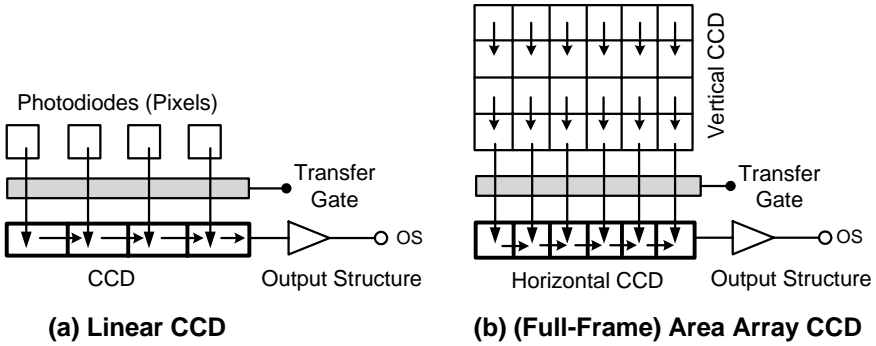


Fig. 2.2. A simplified block diagram of the two fundamental CCD sensor architectures. The arrows denote the movement of the charge packets, facilitated by the clocking signals (adapted from [11])

in Fig. 2.3. At the lower edge of the VCCD array, a single horizontal CCD register (HCCD) is used to combine the outputs from the VCCD into a single output (refer to Fig. 2.2(b)). An additional transfer gate is positioned between the horizontal register and the vertical registers to prevent a charge transfer into the horizontal register, while it is being emptied [11]. During the imaging operations, images are optically projected onto the VCCD array which acts as an image plane. The sensor takes the scene information and partitions the image into discrete elements which are defined by the number of pixels, thus “quantizing” the scene. The resulting rows of the scene information are shifted in a parallel fashion to the serial HCCD register, which subsequently shifts the row of information to the output as a serial stream of data. The process iterates until all the rows of the VCCD are transferred off

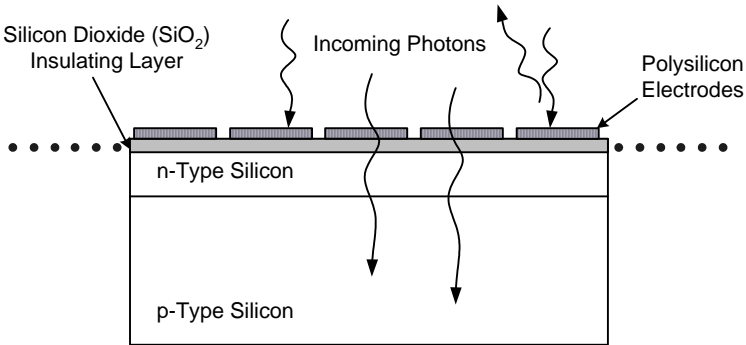


Fig. 2.3. A cross-section of a front-illuminated photogate-based area-array CCD sensor

chip. The image is then reconstructed as dictated by the camera system [13]. Area array CCD sensors are common in consumer digital cameras.

Conventional CCDs are designed for the front-illuminated mode of operation, as depicted in Fig. 2.3. Front-illuminated CCDs are quite economical to manufacture by using standard wafer fabrication procedures, and are popular in consumer imaging applications, as well as industrial-grade applications. However, front-illuminated CCDs are inefficient at short wavelengths (e.g., blue and UV) due to the absorption of photons by the polysilicon layers, if photogates are used as the pixel element. For the front-illuminated area array CCD in Fig. 2.3, the presence of the gate structure (and passivation layers) make it difficult for the short wavelength photons to penetrate the Si substrate, since photons can be absorbed and lost in these upper layers. Furthermore, because of the high absorption coefficient for short wavelength photons in Si and in the overlying materials (e.g., SiO₂, polysilicon), the quantum efficiency (QE) of these front-illuminated CCDs tends to be poor in the blue and UV regions. The gate structure also inhibits the use of an anti-reflective (AR) coating that to boost the QE performance. As a result, the presence of the CCD gates reduces the sensitivity of conventional photogate-based front-illuminated CCDs. Photodiode-based CCDs do not exhibit gate absorption problems due to the absence of the gate (or polysilicon) layers, and offer a higher efficiency at short wavelengths. However, photodiode-based CCDs tend to consume more chip size and may not be suitable for certain applications [13].

Typically, conventional front-illuminated CCDs are adequate for low-end applications and for consumer electronics. But, for large, professional observatories and high-end industrial inspection systems that demand that require extremely sensitive detectors, conventional thick frontside-illuminated chips are rarely used [13]. Thinned back-illuminated CCDs offer a more compatible solution for these applications. Backside-thinned back-illuminated CCDs exhibit a superior responsivity, remarkably in the shorter wavelength region. More details on this design and how it is used to improve UV sensitivity are presented in Sect. 3.3.

Before CCD imaging in UV is examined, the fundamentals of solid-state imaging and the frequently-used terminology for defining the performance of a CCD image sensor are detailed. In particular, QE and dark current are the two key parameters that characterize the CCD behavior in the DUV experiment in Chap. 12. The QE provides a measure of how sensitive the CCD sensor is to incident radiation, and is discussed in Sect. 2.2. Dark current measurements can provide an indication of the extent and type of radiation damage experienced by the sensor. The characteristics and sources of dark current are reviewed in Sect. 2.3. Other parameters such as spectral response, pixel response non-uniformity (PRNU), dark response non-uniformity (DRNU), and charge conversion efficiency (CCE) will also be considered in

this chapter; these parameters will be used to evaluate the DUV-induced damages in CCDs in Chap. 12.

2.1 Fundamentals of Solid-State Imaging

The two fundamental components in a solid-state imaging system are the absorption of photons in the device substrate which cause charge generation, and the collection of the resultant photogenerated charge carriers. The effectiveness of these operations is dependent on the optical and electrical properties of the material and the structure of the device. In this section, these two components are described, and their influence on the parameters such as spectral response and QE are considered in the proceeding section.

2.1.1 Absorption of Photons

The first operation of an imager involves the generation of electric charges from the absorption of incident photons. This is illustrated schematically in Fig. 2.4. The charge generation efficiency (CGE) of a CCD is characterized by the QE, and is dependent on the absorption coefficient of the semiconductor material. When the surface of the semiconducting substrate of the imager is struck by a photon flux, Φ_0 , the absorption of photons is dependent on the photon energy, E_{ph} , in units of eV, given by

$$E_{\text{ph}} = hv = \frac{h \cdot c}{\lambda} = \frac{1.24}{\lambda_{[\mu\text{m}]}} , \quad (2.1)$$

where h is Planck's constant, v is the frequency, λ is the wavelength, and c is the speed of light [12]. The photons are absorbed by the semiconductor if the photon energy is higher than the band-gap energy, E_G , of the semiconductor, expressed mathematically as

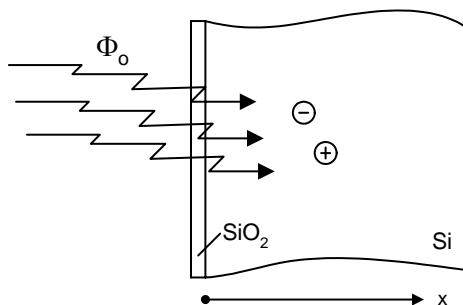


Fig. 2.4. An illustration of the generation of an electron-hole pair due to the impinging photons in the bulk of the silicon (adapted from Theuwissen [12])

$$E_{\text{ph}} \geq E_{\text{G}} , \quad (2.2)$$

The actual photon flux, $\Phi(x)$, at depth x in the substrate, differs from the incoming flux Φ_0 , and is written as

$$\Phi(x) = \Phi_0 e^{-\alpha x} , \quad (2.3)$$

where α is the absorption coefficient of the substrate material. The values of α of the incident radiation are derived by measuring the absorption intensity, I , of a sample with a thickness, x , in cm, as follows:

$$I(x) = I_0 e^{-\alpha x} , \quad (2.4)$$

where I_0 is the intensity of incident light exciting the sample [12]. Equations (2.3) and (2.4) are derived from the Beer-Lambert Law. The absorption characteristics of the semiconducting material can also be described by the penetration depth, x^* . It is defined as the depth at which the remaining photon flux, $\Phi(x^*)$, is equal to e^{-1} or 37% of the incoming flux Φ_0 , and is expressed as

$$\Phi(x^*) = \Phi_0 e^{-1} . \quad (2.5)$$

Thus, the penetration depth and the absorption coefficient appear to have a reciprocal relationship,

$$x^* = \alpha^{-1} . \quad (2.6)$$

The absorption spectrum of Si (i.e., the dependence of the absorption coefficient, α , and the penetration depth, x^* , on the wavelength, λ) is displayed in Fig. 2.5. An inverse dependence exists between α and λ in the visible-IR

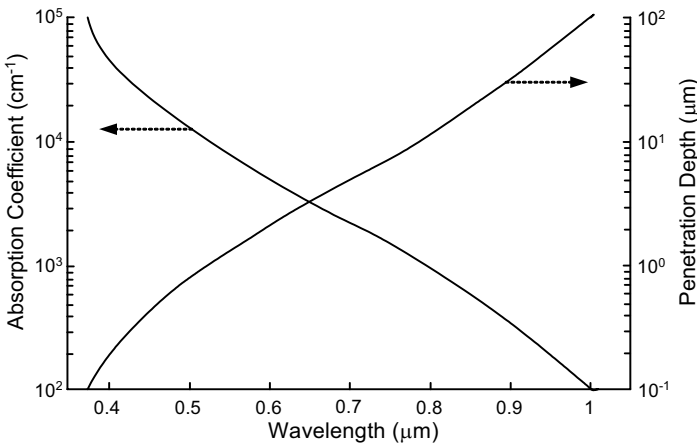


Fig. 2.5. The absorption coefficient and penetration depth of silicon in the visible wavelength spectrum (adapted from Theuwissen [12])

region. This implies that the IR radiation with a longer λ (e.g., 1000 nm) has a smaller α (i.e., a larger x^*) and can penetrate much deeper into the Si before it is absorbed when compared to green light with shorter λ (e.g., 500 nm). For even shorter wavelengths (e.g., blue light), the photon flux is absorbed within a much thinner layer of the Si due to a larger α (i.e., a smaller x^*).

By virtue of the photoelectric effect, the absorption of the photons in the Si results in the generation of electron-hole (e-h) pairs. The amount of charge that is generated depends on the incoming flux, the wavelength of the incoming light, and the absorption coefficient of the semiconducting substrate [12]. For CCD sensors, the charge generation takes place primarily in the Si substrate.

2.1.2 Charge Collection

The other component of a solid-state imaging system is the charge collection. After the generation of the e-h pairs from the absorbed photons, the electrons are separated from the holes within the Si, and collected in the nearest potential well (typically, the depletion region). The CCD cross-section, shown in Fig. 2.1 and Fig. 2.3, contains an n-type Si epitaxial layer on top of a p-type Si substrate, forming a p-n junction that is situated relatively close to the surface of the sensor. An electric field, originating from the depletion region of this p-n junction, causes the e-h pair to separate. All the minority carriers generated in this depletion region are captured by the CCD potential well; thus, the efficiency of charge collection in this region is 100% [12]. However, a portion of the incident photons are absorbed outside the depletion region. For example, some of the photons generate e-h pairs in the neutral bulk of the semiconductor substrate. These carriers in the neutral bulk must diffuse toward the collection site (i.e., the depletion region) in order to contribute to the CCD response. This process of collecting the charges that are generated outside the depletion region relies on the diffusion of the charges to the potential wells; this process has lower efficiency if the diffusion length of the minority carriers is too short, because the charge carriers can be lost by recombination.

The total efficiency of the charge collection process, η_c , for the imager is described as follows:

$$\eta_c = \eta_{\text{dl}} + \eta_{\text{bulk}} , \quad (2.7)$$

where the collection in the depletion layer is described by η_{dl} and in the neutral bulk by η_{bulk} [12]. The collection efficiency, η_c , depends on the wavelength of the incident photons and the absorption characteristics of the material. In the case of longer wavelength photons, they have lower absorption coefficients and are likely to have less absorption in the depletion region. As a result, the overall collection efficiency is more heavily dependent on the bulk characteristics of the Si; thus, a longer diffusion length favors a higher collection efficiency for irradiation at long wavelengths. In the case of shorter visible wavelength photons, they are more likely to be absorbed in the depletion